Implementation of the ATLAS-SUSY-2019-08 analysis in the MadAnalysis 5 framework

MARK D. GOODSELL

Laboratoire de Physique Théorique et Hautes Energies (LPTHE),
UMR 7589, Sorbonne Université et CNRS, 4 place Jussieu, 75252 Paris Cedex 05, France.

This is the validation note for the recast in MadAnalysis 5 of the study ATLAS-SUSY-2019-08: a search for direct production of electroweakinos in final states with one lepton, missing transverse momentum and a Higgs boson decaying into two b-jets in pp collisions at $\sqrt{s} = 13$ TeV with the ATLAS detector, using an integrated luminosity of $139\,\text{fb}^{-1}$. The recasting code is validated against cutflows and expected signal events for benchmark scenarios, and the exclusion limits are reproduced for a simplified supersymmetric electroweakino sector consisting of a degenerate wino decaying to a light stable bino.

1. Introduction

This note describes the recasting of the study ATLAS-SUSY-2019-08 [1] in MadAnalysis 5 [2,3], and available in the Public Analysis Database [4,5]. This analysis targets electroweakinos produced in the combination of a chargino and a heavy neutralino, where the neutralino decays by emitting an on-shell Higgs, and the chargino decays by emitting a W boson. The Higgs is identified by looking at b-jets with an invariant mass in the window $[100, 140]$ GeV, while the W boson is identified through leptonic decays. The typical production diagram targeted via the search is shown in figure 1. The analysis uses $139\,\text{fb}^{-1}$, and is well adapted to search for a relatively flavour-pure wino that can decay to a bino (winos being the fermionic superpartner of W-bosons, binos being the partners of the hypercharge, and if they are flavour-pure there is little mixing between the states) with a moderate-to-large mass splitting between the two, since a wino has a large production cross-section, and would occur as a roughly degenerate chargino/neutralino pair.

This search should be particularly effective when other supersymmetric particles (such as sleptons and additional Higgs fields) are heavy; there are other, specifically adapted searches for those cases. However, given constraints on heavy Higgs sectors and colourful particles, this analysis is rather model independent and difficult to evade in a minimal model. The assumption of chargino decay via a W boson is indeed rather a good one, it should proceed typically with branching ratio close to unity, provided: (a) that there is no charged Higgs or slepton channel available, (b) the decay is kinematically allowed, and (c) the chargino is relatively pure wino (with small higgsino component). If we relax assumption (a), then the cascade decay is preferred; if we relax (b) then three-body and loop decays are preferred; if we relax assumption (c) then the decay channel via a Z boson would also have a significant branching ratio.

The ATLAS collaboration made available substantial additional data via HepData [6] at https://www.hepdata.net/record/ins1755298, in particular including detailed cutflows and tables for the exclusion curves, and full likelihoods, which are relevant for this note. For simplified model analysis they also provided efficiency maps.

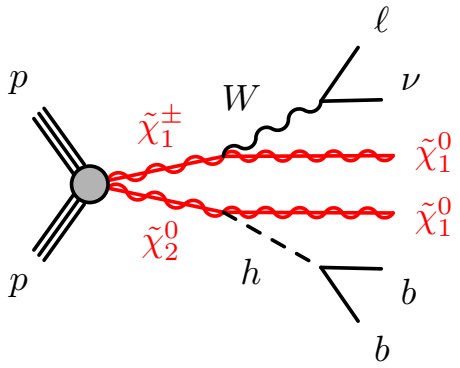

Fig. 1. The signal scenario targeted by [1], taken from that paper. Note that the simulated signal events also include up to two hard jets not shown here.

2. Preselection and event cleaning

This analysis has a number of preselection cuts on the events; I shall first summarise them as presented in the ATLAS paper and in the provided pseudocode; in subsection 2.2 I will describe how these are implemented in the recasting code.

2.1. *Selections defined in the ATLAS paper*

Jets are reconstructed from using the anti-k_t algorithm with a radius parameter $R = 0.4$ [7], and this is done internally in DELPHES 3 [8] using FASTJET [9]. Initial 'soft' jets are selected in the region $|\eta| < 4.5$ and have $p_T > 20$ GeV; initial 'soft' leptons are defined according to the baseline kinematic and isolation criteria listed in appendix Appendix A (where the criteria for signal lepton isolation are also given). To suppress jets from pile-up interactions, the jets with $|\eta| < 2.8$ and $p_T < 120$ GeV are required to satisfy the 'medium' working point of the jet vertex tagger (JVT), a tagging algorithm that identifies jets originating from the Primary Vertex (PV) using track information.

Next, an overlap removal procedure is applied to electrons, muons and jets. First, for overlapping electrons, the electron with the lower p_T is rejected; and any electron overlapping with a muon is rejected (the criterion for overlap is interpreted in the provided pseudocode and therefore in the recasting code as having $\Delta R < 0.01$). Next, electrons and muons within a cone of size $\Delta R = \min(0.4, 0.04 + 10\ \text{GeV}/p_T)$ around a jet are removed, and jets are rejected if they lie within $\Delta R = 0.2$ of a muon. The remaining objects constitute the *baseline* leptons and jets.

From the baseline objects, signal jets are required to be in the region $|\eta| < 2.8$ and have $p_T > 30$ GeV, and of these, b-tagged signal jets are reconstructed with $|\eta| < 2.5$[a].

2.2. *Implementation of preselection*

This recast relies on detector simulation through DELPHES [8] with a specially modified card. There are several issues with the standard ATLAS card, uncovered when comparing with the experimental

[a]The first version of the analysis paper incorrectly gave $p_T > 20$ GeV for the b-jets.

cutflows:

- The isolation options are too simple (only a fixed ΔR is possible).
- Too few signal leptons and jets are reconstructed with the given efficiencies. In particular, the kinematic selections on leptons start at 6 GeV, whereas the standard reconstruction efficiencies are zero below 10 GeV.
- It is not possible to distinguish between "background" and "signal" leptons in terms of whether they should be clustered with jets. In ATLAS, leptons identified as coming from hadronic decays (so usually clustered into a jet and/or having a displaced vertex associated with e.g. charged pion decays) are designated "background" and not considered as part of the baseline leptons. In Delphes, if we use the isolation routines, the "unique object identifier" will decide whether a lepton is part of a jet depending on whether it is isolated – but isolation criteria prove to be inadequate for this job for this analysis, removing too few leptons.
- The b-tag algorithm used (MV2c10) has a quoted efficiency 77% independent of p_T; it is not clear how this corresponds to the Delphes b-tagging, but certainly the "standard" efficiency is much worse than this. Unfortunately, it also appears that even setting a flat 77% efficiency of b-tagging also results in too few b-jets.
- There is no default implementation of the jet vertex tagging algorithm in Delphes. This complicates the situation regarding pile-up: if we include pile-up events in Delphes, then we will have the wrong number of jets unless we also implement a jet vertex tagger in the analysis.

To solve these issues, I modified the Delphes card and implemented several features directly in the analysis:

- Electron, muon and photon reconstruction and tracking efficiencies were modified to reflect the improved performance of ATLAS, e.g. given in [10, 11].
- ΔR for jet reconstruction was set to 0.4 as used in the analysis.
- The Hadron calorimeter (HCAL) minimum energy and energy significance are halved; this way more jets are found and the m_T distribution better matches the cutflows.
- For b-tagging, a flat 77% efficiency is taken for $p_T > 300$ GeV to match the MC2c10 result. For smaller values, 85% is taken. This was done after investigating b-tagging performance for $t\bar{t}$ processes and comparing to truth jets; I found that for $p_T \lesssim 300$ GeV the b-tagging efficiency in Delphes was poor. This certainly warrants further investigation.
- Isolation is deactivated in the Delphes card and implemented directly in the analysis. This also means that we must identify leptons/photons uniquely in the analysis, through a function labelled `RemoveFakeJets`, very similar to the inbuilt MadAnalysis 5 function `JetCleaning`.
- To emulate the JVT and effect of pileup, efficiencies are implemented *in the analysis* for jets with $|\eta| < 2.8$ and for $p_T < 120$ GeV with $|\eta| < 2.5$. Removed jets have their momentum added to missing p_T. In addition, jets missing the baseline criteria and having $|\eta| > 2.5$ add their momentum to missing p_T, because they cannot contribute to the "soft term" defined in the analysis.
- To remove "background" leptons, since we cannot access jet constituents in MadAnalysis 5 (and so determine whether a lepton is clustered with a jet) I use as a proxy the absolute displacement of the lepton creation vertex, in addition to the isolation criteria defined in the analysis and given in the appendix. I define any electron or muon created more than 0.1 mm

from the primary vertex as "background" and removed. This is similar to the algorithm used by the experiments which look for the characteristic "kink" [10] but with a (presumably) unrealistically small cutoff; this is unfortunately the best that can be done in the current framework. It therefore misses a few prompt decays from *neutral* pions (which have only a very small branching ratio to electrons so this is not a problem) but is potentially dangerous in models with non-prompt chargino decays so this analysis should be used with caution in such cases.

Once these have been applied, I then apply the cuts described in the analysis and recalled in the next section.

3. Signal regions and data

	SR-LM	**SR-MM**	**SR-HM**
N_{lepton}	$= 1$		
p_T^ℓ [GeV]	$> 7(6)$ for $e(\mu)$		
N_{jet}	$= 2$ or 3		
$N_{b\text{-jet}}$	$= 2$		
E_T^{miss}[GeV]	> 240		
m_{bb}[GeV]	$\in [100, 140]$		
$m(\ell, b_1)$ [GeV]	–	–	> 120
m_{T}[GeV] (excl.)	$\in [100, 160]$	$\in [160, 240]$	> 240
m_{CT}[GeV] (excl.)	$\{\in [180, 230], \in [230, 280], > 280\}$		
m_{T}[GeV] (disc.)	> 100	> 160	> 240
m_{CT}[GeV] (disc.)	> 180		

Table 1: Overview of the selection criteria for the signal regions. Each of the three 'excl.' SRs is binned in three m_{CT} regions.

The signal regions are summarised in table 1. There are therefore 12 signal regions, which are denoted in the recasting code as `XXdisc, XXlowCT, XXmedCT, XXhighCT` for `XX` $\in$ { `LM,MM,HM` } respectively corresponding to the **SR-LM**, **SR-MM**, **SR-HM** in the table. They are split into two categories: "disc." (for "discovery") and "excl." (for "exclusion") which are not independent (as discussed below). In the cuts, several quantities are defined:

- The invariant mass of the two b-jets, m_{bb}. This targets the main decay channel of the SM Higgs boson.
- $m(\ell, b_1)$, which is the invariant mass of the lepton and the leading b-jet.
- The transverse mass m_{T} is given in the analysis paper as:

$$m_{\text{T}} = \sqrt{2p_{\text{T}}^\ell E_T^{\text{miss}}(1 - \cos[\Delta\phi(\boldsymbol{p}_{\text{T}}^\ell, p_T^{\text{miss}})])},$$

where $\Delta\phi(\boldsymbol{p}_{\text{T}}^\ell, p_T^{\text{miss}})$ is the azimuthal angle between $\boldsymbol{p}_{\text{T}}^\ell$ and p_T^{miss}. This is not the same as the definition in [12,13] cited by the analysis, only applying when the lepton is massless. Since the pseudocode provided with the analysis uses a predefined hidden function for the transverse mass, I choose to use the full expression in the analysis even if the effect is irrelevant.

- The contransverse mass of two b-jets, $m_{\rm CT}$, is defined as:

$$m_{\rm CT} = \sqrt{2p_T^{b_1} p_T^{b_2} (1 + \cos\Delta\phi_{bb})},$$

where $p_T^{b_1}$ and $p_T^{b_2}$ are the transverse momenta of the two leading b-jets and $\Delta\phi_{bb}$ is the azimuthal angle between them. Again this differs from the cited definition in [12, 13], being equal only when the b-jets are massless. Once again I implemented the function including masses.

The analysis also provides sample cutflows (to which I compare results in section 5) which introduce additional cuts. Most of these are self-explanatory, and I implement them in the same order in the recasting; however, the first cut is simply labelled "$N_{\rm jets,25} \geq 2$" which I interpret as being two jets with $p_T \geq 25$ GeV. An alternative interpretation would be $|\eta| < 2.5$; since the analysis requires two or three signal jets with $p_T > 30$ and two b-jets with $|\eta| < 2.5$ these choices make no difference to the final efficiency, and, since there was some difficulty matching the initial number of jets, I take the more permissive choice.

SR-LM	LMdisc	LMlowCT	LMmedCT	LMhighCT
Observed	66^*	16	11	7
Expected	$47^* \pm 6^*$	8.8 ± 2.8	11.3 ± 3.1	7.3 ± 1.5
SR-MM	MMdisc	MMlowCT	MMmedCT	MMhighCT
Observed	32^*	4	7	2
Expected	$20.5^* \pm 4^*$	4.6 ± 1.7	2.6 ± 1.3	1.4 ± 0.6
SR-HM	HMdisc	HMlowCT	HMmedCT	HMhighCT
Observed	14	6	5	3
Expected	8.1 ± 2.7	4.1 ± 1.9	2.9 ± 1.3	1.1 ± 0.5

Table 2: Expected background and observed events for each signal region, taken from Table 5 of [1] for the exclusion regions and HMdisc; for LMdisc and MMdisc the data were scraped from Figure 4 of that reference (and are hence labelled with an asterisk), since tabulated data were not provided.

The observed and expected background events for each signal region are reproduced in table 2. The "disc." (for "discovery") regions are supposed to be for "discovery and model-independent limits" but are not independent of the other regions. The HMdisc region is the sum of all HM bins, and LMdisc includes all of the MMdisc bins as a subset. However, the LMdisc and MMdisc regions cannot be obtained from the exclusion regions, due to the $m(\ell, b_1)$ cut on the HM bins which does not apply to them. ATLAS only use the exclusion bins for setting limits in their exclusion plot; moreover, the discovery regions have excesses, and since the data is not precisely available I do not include it in the "info" card for the analysis so that it will not interfere with the setting of limits. However, if the user wants to use these regions, I also provide a card `atlas_susy_2019_08_with_disc_regions.info` which includes them.

4. Generation of signal events

The signal events simulated in [1] assume a simplified model with wino-like $\tilde{\chi}_2^0/\tilde{\chi}_1^+$ which are degenerate and decay to a bino-like lightest supersymmetric particle (LSP) $\tilde{\chi}_1^0$. The branching ratios of the decays $\tilde{\chi}_2^0 \to \tilde{\chi}_1^0 + h, \tilde{\chi}_1^+ \to \tilde{\chi}_1^0 + W_\mu^+$ are taken to be 100%, which, as described above, may not be far from realistic, although the scenario as a whole would be disfavoured as having an unrealistic relic density of dark matter. On the other hand, in the signal events, the decay $h \to bb$ and $W^+ \to \ell\nu$ are specifically selected; in the SM these rates are 58.3% and 10.86% to $\mu^+\nu_\mu$, 10.71% to $e^+\nu_e$, so if we naively simulated a general hard process and shower with the full decay table, then we would only be targeting about 12% of the points before any other cuts are applied.

To reproduce the signal events from [1], I used the standard MSSM UFO [14] file for the MSSM [15, 16] included with MadGraph5_aMC@NLO`v2.8` [17] and spectrum files provided as auxiliary material by the analysis. The hard process is simulated in MadGraph5_aMC@NLO`v2.8` and showering is performed in Pythia8 [18], with detector response simulated in Delphes [8] using a card modified as described above. The analysis uses the A14 Pythia tune [19], so I include those changes in the Pythia8 card (summarised in appendix Appendix B) in addition to the choices:

```
24:offIfAny=1 2 3 4 5 6 15 16
25:oneChannel=1 0.5876728 0 -5 5
```

These select the W decays to electrons/muons, and Higgs decays to b-quarks, while allowing Pythia8 to use its inbuilt routines for the phase-space of the decays, rather than using a flat phase-space as would be the case for SLHA decay blocks. Note that this is not the only way the filters could be used in Pythia8, however in MadGraph5_aMC@NLO the commands are read and then reordered alphabetically (and, in fact, earlier versions would not recognise these sorts of commands) so some care is needed to make sure that only one command per particle is passed!

The simulated signal events in [1] involve up to two hard jets, which are then merged with the CKKL algorithm [20] with a merging scale of one quarter the mass of the $\tilde{\chi}_1^\pm/\tilde{\chi}_2^0$. In the analysis below, I take the default MLM merging algorithm [21, 22] used in MadGraph5_aMC@NLO, but there the paremeter `xqcut` is used to set the merging scale:

$$\texttt{qcut} = \frac{3}{2}\texttt{xqcut} \longrightarrow \texttt{xqcut} = m_{\tilde{\chi}_1^\pm}/6. \tag{4.1}$$

To match the cutflows provided, I simulated 150k events at leading order in MadGraph5_aMC@NLO, which after merging and passing to Pythia8 give between 100k and 120k merged events depending on the point; for a comparison of the exclusion plot I use 100k events per point. Both the ATLAS analysis and this recasting use the `NNPDF2.3LO` parton distribution functions (pdfs).

ATLAS use NLO-NLL cross-sections, and so to match the final number of events I interpolate the cross-sections from [23–26] tabulated at

https://twiki.cern.ch/twiki/bin/view/LHCPhysics/SUSYCrossSections13TeVn2x1wino

For other models, the user should use the leading-order *merged* cross-sections unless an improved calculation is available. As an example of the impact of the NLO/NLL corrections, the cross-sections

for the example cutflow points are:

$(m(\tilde{\chi}_1^\pm, \tilde{\chi}_1^0)$[GeV]	σ^{LO}(fb)	$\sigma^{NLO-NLL}$(fb)
$(300, 75)$	278	387 ± 26
$(500, 0)$	31.8	46.4 ± 4.2
$(750, 100)$	4.5	6.7 ± 0.8

(4.2)

The corrections are therefore consistently around 40% to 50%.

5. Cutflows

To validate the recasting, I present here the cutflows compared to all of the examples given in the HepData repository [6]. The cutflows are weighted to match the final number of events predicted, and helpfully include uncertainties.

To compare the cutflows from [1] with the recasting presented here, I define the net efficiency of each cut by

$$\begin{aligned} \epsilon_i^{\rm MA} \equiv & \frac{\text{sum of weights of events surviving cut } i}{\text{sum of weights of merged events}}, \\ \epsilon_i^{\rm ATLAS} \equiv & \frac{\text{number of simulated events surviving cut } i}{\text{initial number of weighted events (after cleaning)}}. \end{aligned} \tag{5.1}$$

The analysis also provide uncertainties for their data, which I translate into uncertainties on the efficiency, while for the implementation here I can only calculate Monte-Carlo errors given by

$$\sigma(\epsilon_i^{\rm MA}) = \sqrt{\frac{\epsilon_i^{\rm MA}(1-\epsilon_i^{\rm MA})}{N}}, \tag{5.2}$$

where N is the initial number of merged events before cuts. In tables 3,4,5 I give the cutflow comparisons for all available signal regions and list in the final column the percentage error of each cut compared to those provided by ATLAS, defined as

$$\delta_i \equiv \frac{\epsilon_i^{\rm MA} - \epsilon_i^{\rm ATLAS}}{\epsilon_i^{\rm ATLAS}} \times 100. \tag{5.3}$$

I find very good agreement (to within one standard deviation of the ATLAS result) for each cutflow, with the possible exception of the medium CT bins for the LM and MM points, where the results agree within two standard deviations. Indeed, the points with the poorest agreement also have the largest experimental uncertainties.

For each point, I also compare the final number of events passing all cuts. This is given as

$$\begin{aligned} \text{Number of events (MA)} = & 139\,\text{fb}^{-1} \times \sigma(pp \to \tilde{\chi}_1^\pm + \tilde{\chi}_2^0 + nj, n \leq 2) \\ & \times \epsilon_{\rm final}^{\rm MA} \times 0.583 \times 0.2157, \end{aligned} \tag{5.4}$$

where $\epsilon_{\rm final}^{\rm MA}$ refers to the efficiency of the final cut, σ is the cross-section for the hard process (obtained from [23–26] as described above), and the final two factors account for the SM ratio of $H \to bb$ and $W \to \ell\nu$. This number, along with the ATLAS value, is given alongside the cutflows in tables 3-5, with the Monte-Carlo uncertainty (from "only" simulating 150k events) and the cross-section uncertainty given separately.

LM preselection cuts			
Cut	$\epsilon_i^{\rm ATLAS}$	$\epsilon_i^{\rm MA}$	δ_i
$N_{\rm jets,25} \geq 2$	0.8116 ± 0.0000	0.7502 ± 0.0014	-7.6%
1 signal lepton	0.7053 ± 0.0000	0.6205 ± 0.0016	-12.0%
Second baseline lepton veto	0.6868 ± 0.0000	0.6205 ± 0.0016	-9.7%
$m_{\rm T} > 50$ GeV	0.5601 ± 0.0000	0.4928 ± 0.0016	-12.0%
$E_{\rm T}^{\rm miss} > 180$ GeV	0.1639 ± 0.0000	0.1341 ± 0.0011	-18.2%
$N_{\rm jets} \leq 3$	0.1399 ± 0.0033	0.1135 ± 0.0010	-18.9%
$N_{\rm b-jets} = 2$	0.0575 ± 0.0022	0.0520 ± 0.0007	-9.5%
$m_{\rm bb} > 50$ GeV	0.0575 ± 0.0022	0.0509 ± 0.0007	-11.4%
$E_{\rm T}^{\rm miss} > 240$ GeV	0.0228 ± 0.0013	0.0213 ± 0.0005	-6.5%
$m_{\rm bb} \in$ [100,140] GeV	0.0175 ± 0.0012	0.0156 ± 0.0004	-10.6%
Region LMdisc			
$m_{\rm T} > 100$ GeV	0.0123 ± 0.0010	0.0115 ± 0.0003	-6.6%
$m_{\rm CT} > 180$ GeV	0.0097 ± 0.0008	0.0084 ± 0.0003	-12.8%
Number of events (ATLAS):	58.0 ± 5.0		
Number of events (MA):	57.0 $\pm$2.0 (stat) $\pm$3.9 (xsec)		
Region LMlow			
$m_{\rm T} \in$ [100,160] GeV	0.0050 ± 0.0007	0.0045 ± 0.0002	-10.5%
$m_{\rm CT} \in$ [180,230] GeV	0.0010 ± 0.0003	0.0007 ± 0.0001	-30.4%
Number of events (ATLAS):	6.2 ± 1.7		
Number of events (MA):	4.9 $\pm$0.6 (stat) $\pm$0.3 (xsec)		
Region LMmed			
$m_{\rm T} \in$ [100,160] GeV	0.0050 ± 0.0007	0.0045 ± 0.0002	-10.5%
$m_{\rm CT} \in$ [230,280] GeV	0.0017 ± 0.0004	0.0011 ± 0.0001	-39.1%
Number of events (ATLAS):	10.5 ± 2.2		
Number of events (MA):	7.2 $\pm$0.7 (stat) $\pm$0.5 (xsec)		
Region LMhigh			
$m_{\rm T} \in$ [100,160] GeV	0.0050 ± 0.0007	0.0045 ± 0.0002	-10.5%
$m_{\rm CT} > 280$ GeV	0.0018 ± 0.0004	0.0020 ± 0.0001	13.8%
Number of events (ATLAS):	10.6 ± 2.3		
Number of events (MA):	13.6 $\pm$1.0 (stat) $\pm$0.9 (xsec)		

Table 3: Cutflow comparison for Low Mass signal regions.

6. Comparison of exclusion plot

To make a final comparison of the recasting quality, I also present a reconstruction of the excluded region in the $m_{\tilde{\chi}_2^0}$–$m_{\tilde{\chi}_1^0}$ plane using the procedure outlined above, by simulating a selection of points at given masses marked in the plot, and comparing to the contour from [1]. A point is considered excluded if $1 - {\rm CL}_s > 0.95$, where ${\rm CL}_s$ is determined by the procedure in [28] and implemented in MadAnalysis 5. As per the default MadAnalysis 5 procedure, the ${\rm CL}_s$ value is computed separately

MM preselection cuts			
Cut	$\epsilon_i^{\text{ATLAS}}$	ϵ_i^{MA}	δ_i
$N_{\text{jets},25} \geq 2$	0.8666 ± 0.0000	0.7859 ± 0.0012	-9.3%
1 signal lepton	0.7598 ± 0.0000	0.6784 ± 0.0014	-10.7%
Second baseline lepton veto	0.7370 ± 0.0000	0.6784 ± 0.0014	-7.9%
$m_{\text{T}} > 50$ GeV	0.6531 ± 0.0000	0.5951 ± 0.0015	-8.9%
$E_{\text{T}}^{\text{miss}} > 180$ GeV	0.4574 ± 0.0000	0.3943 ± 0.0015	-13.8%
$N_{\text{jets}} \leq 3$	0.3837 ± 0.0089	0.3465 ± 0.0014	-9.7%
$N_{\text{b-jets}} = 2$	0.1601 ± 0.0051	0.1778 ± 0.0012	11.1%
$m_{\text{bb}} > 50$ GeV	0.1588 ± 0.0051	0.1751 ± 0.0011	10.3%
$E_{\text{T}}^{\text{miss}} > 240$ GeV	0.1131 ± 0.0051	0.1236 ± 0.0010	9.3%
$m_{\text{bb}} \in [100,140]$ GeV	0.0865 ± 0.0042	0.0896 ± 0.0009	3.5%
Region MMdisc			
$m_{\text{T}} > 160$ GeV	0.0665 ± 0.0037	0.0691 ± 0.0008	4.0%
$m_{\text{CT}} > 180$ GeV	0.0485 ± 0.0032	0.0494 ± 0.0007	1.8%
Number of events (ATLAS):	38.2 ± 2.5		
Number of events (MA):	40.0 $\pm$0.5 (stat) $\pm$3.6 (xsec)		
Region MMlow			
$m_{\text{T}} \in [160,240]$ GeV	0.0161 ± 0.0018	0.0143 ± 0.0004	-11.6%
$m_{\text{CT}} \in [180,230]$ GeV	0.0033 ± 0.0008	0.0025 ± 0.0001	-25.5%
Number of events (ATLAS):	2.6 ± 0.6		
Number of events (MA):	2.0 $\pm$0.1 (stat) $\pm$0.2 (xsec)		
Region MMmed			
$m_{\text{T}} \in [160,240]$ GeV	0.0161 ± 0.0018	0.0143 ± 0.0004	-11.6%
$m_{\text{CT}} \in [230,280]$ GeV	0.0043 ± 0.0009	0.0029 ± 0.0002	-32.1%
Number of events (ATLAS):	3.4 ± 0.7		
Number of events (MA):	2.4 $\pm$0.1 (stat) $\pm$0.2 (xsec)		
Region MMhigh			
$m_{\text{T}} \in [160,240]$ GeV	0.0161 ± 0.0018	0.0143 ± 0.0004	-11.6%
$m_{\text{CT}} > 280$ GeV	0.0069 ± 0.0011	0.0075 ± 0.0003	9.0%
Number of events (ATLAS):	5.4 ± 0.9		
Number of events (MA):	6.1 $\pm$0.2 (stat) $\pm$0.5 (xsec)		

Table 4: Cutflow comparison for Medium Mass signal regions.

for each *exclusion* signal region, *excluding the discovery regions*[b] (as discussed in section 3), using the data in table 2, and the limit is taken from the signal region which has the smallest *expected* 95% confidence-level limit on the cross-section (that is, treating the observed number of events as equal to the expected background) for regions where the efficiency of the signal is not zero. We see that the exclusion contour from [1] is reasonably well reconstructed by the recasting presented here.

[b]I investigated including the discovery regions, and found worse agreement with the experimental plot, including in particular non-excluded points at lower masses since the region LMdisc has an excess.

HM preselection cuts			
Cut	$\epsilon_i^{\rm ATLAS}$	$\epsilon_i^{\rm MA}$	δ_i
$N_{\rm jets,25} \geq 2$	0.8833 ± 0.0000	0.7975 ± 0.0012	-9.7%
1 signal lepton	0.7917 ± 0.0000	0.7003 ± 0.0013	-11.5%
Second baseline lepton veto	0.7667 ± 0.0000	0.7003 ± 0.0013	-8.7%
$m_{\rm T} > 50$ GeV	0.7083 ± 0.0000	0.6413 ± 0.0014	-9.5%
$E_{\rm T}^{\rm miss} > 180$ GeV	0.6083 ± 0.0000	0.5301 ± 0.0014	-12.9%
$N_{\rm jets} \leq 3$	0.5092 ± 0.0117	0.4680 ± 0.0014	-8.1%
$N_{\rm b-jets} = 2$	0.2258 ± 0.0075	0.2459 ± 0.0012	8.9%
$m_{\rm bb} > 50$ GeV	0.2250 ± 0.0075	0.2432 ± 0.0012	8.1%
$E_{\rm T}^{\rm miss} > 240$ GeV	0.1917 ± 0.0075	0.2072 ± 0.0012	8.1%
$m_{\rm bb} \in$ [100,140] GeV	0.1450 ± 0.0067	0.1502 ± 0.0010	3.6%
$m_{\ell,{\rm b}_1} > 120$ GeV	0.1350 ± 0.0058	0.1383 ± 0.0010	2.5%
$m_{\rm T} > 240$ GeV	0.0967 ± 0.0050	0.1022 ± 0.0009	5.7%
Region HMdisc			
$m_{\rm CT} > 180$ GeV	0.0842 ± 0.0050	0.0868 ± 0.0008	3.2%
Number of events (ATLAS):	10.1 ± 0.6		
Number of events (MA):	10.2 $\pm$0.1 (stat) $\pm$1.2 (xsec)		
Region HMlow			
$m_{\rm CT} \in$ [180,230] GeV	0.0158 ± 0.0021	0.0149 ± 0.0003	-5.6%
Number of events (ATLAS):	1.9 ± 0.2		
Number of events (MA):	1.7 $\pm$0.0 (stat) $\pm$0.2 (xsec)		
Region HMmed			
$m_{\rm CT} \in$ [230,280] GeV	0.0182 ± 0.0022	0.0175 ± 0.0004	-4.3%
Number of events (ATLAS):	2.2 ± 0.3		
Number of events (MA):	2.0 $\pm$0.0 (stat) $\pm$0.2 (xsec)		
Region HMhigh			
$m_{\rm CT} > 280$ GeV	0.0500 ± 0.0042	0.0545 ± 0.0007	9.0%
Number of events (ATLAS):	6.0 ± 0.5		
Number of events (MA):	6.4 $\pm$0.1 (stat) $\pm$0.7 (xsec)		

Table 5: Cutflow comparison for High Mass signal regions.

On the other hand, for this analysis, full likelihoods are available in HepData [6], and so I make use of them via a private code adapted from the approach in `SModelS` [29]. The background-only likelihood contains data for the exclusion signal regions, so I patch it with the expected number of events for each of these, and remove the "other" (CR/VR) regions, and compute the CL_s value with `pyhf` [27]. The results are shown in figure 3, which shows a very good agreement with the experimental plot. Since a future update of MadAnalysis 5 will include a separate implementation of this calculation and a more thorough investigation for this analysis, I do not provide my code with this analysis. However, we see from the two comparisons that the full likelihood calculation gives a much better agreement for the exclusion contour, increasing the reach in $m_{\tilde{\chi}_1^0}$ from 200 GeV to 250 GeV – although the reach on the mass of $m_{\tilde{\chi}_1^\pm}/m_{\tilde{\chi}_2^0}$ is not much affected.

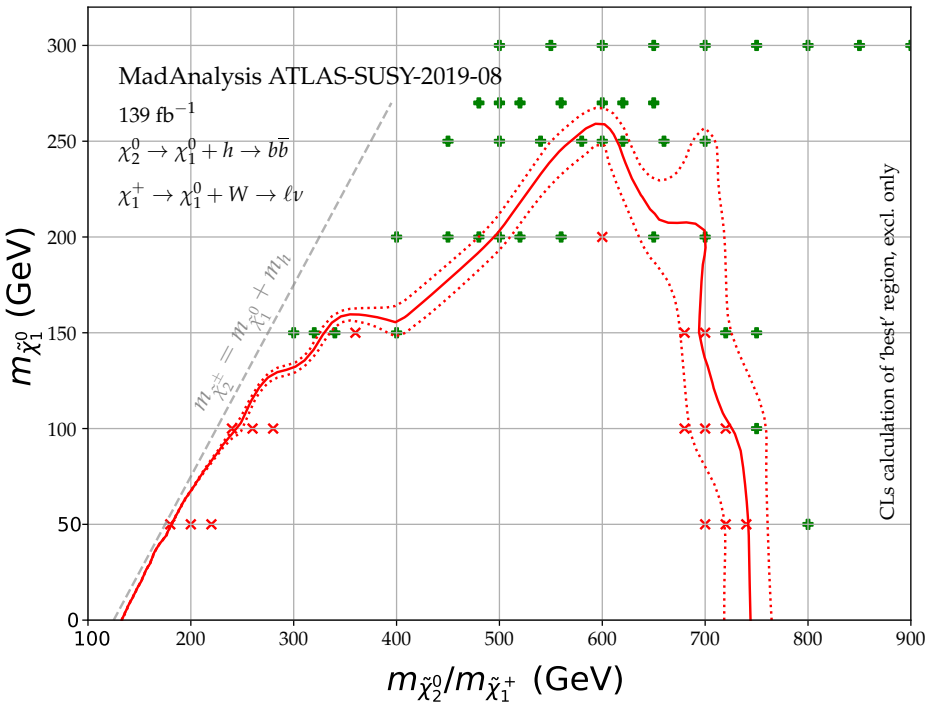

Fig. 2. Comparison of experimental exclusion contour (solid red line; dotted lines are the $\pm 1\sigma$ variation) provided in HepData with the points simulated and tested with this analysis, using the standard MadAnalysis 5 procedure for setting limits based on the "best" region. Points excluded at $1 - \mathrm{CL}_s > 0.95$ are marked with red crosses; non-excluded points are shown as green plusses.

7. Conclusions

The recast described in this note, implemented in the MadAnalysis 5 framework and using fast detector simulation through Delphes with a custom card, can well reproduce the experimental cutflows and exclusion plot for a wino-like electroweakino decaying to a bino-like lightest neutralino. The code is available online from the MadAnalysis 5 dataverse [5], at https://doi.org/10.14428/DVN/BUN2UX, which also includes the custom Delphes and Pythia8 cards. The code described here can therefore be applied to other models/scenarios, as was done using an early version in [30] in the Minimal Dirac Gaugino Model, with the caveat that only promptly decaying particles will be reliably constrained (due to the method employed to eliminate "background" leptons). I also identified several other areas for future investigation: improvements in modelling the b-tagging, jet reconstruction efficiency, isolation, JVT and the missing energy calculation, in order to accurately match recast analyses to recent ATLAS studies.

Acknowledgments

MDG acknowledges support from the grant "HiggsAutomator" of the Agence Nationale de la Recherche (ANR) (ANR-15-CE31-0002). I thank Sabine Kraml, Sophie Williamson and Humberto Gonzales Reyes for collaboration on a related project using this analysis; and Jack Araz and Benjamin Fuks for helpful discussions and comments on the draft.

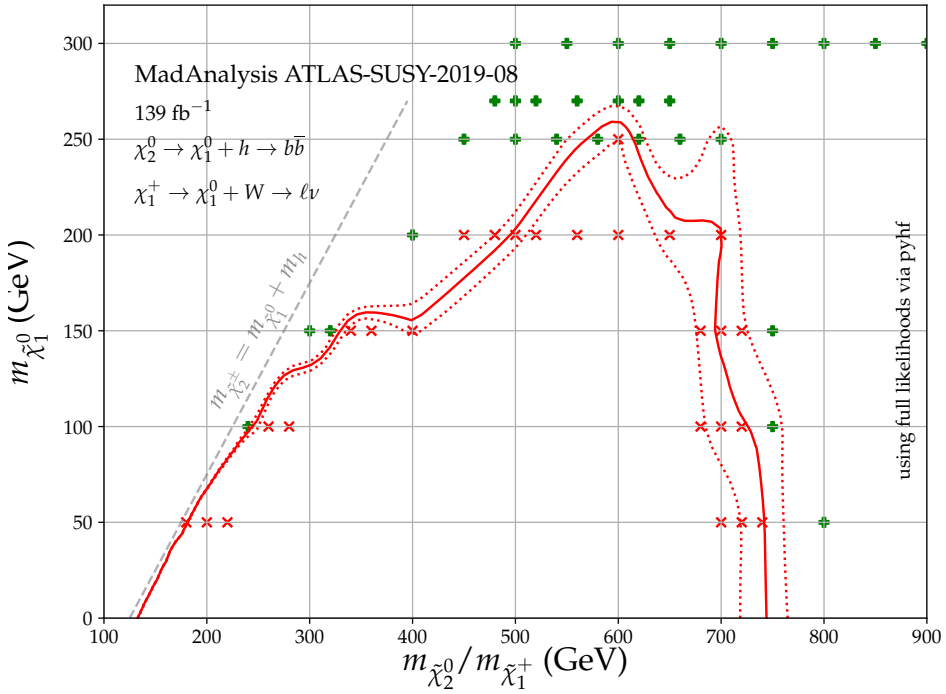

Fig. 3. Comparison of experimental exclusion contour (solid red line; dotted lines are the $\pm 1\sigma$ variation) provided in HepData with the points simulated and tested with this analysis, with statistics calculated using `pyhf` [27] and the provided background likelihood. Points excluded at $1 - \mathrm{CL}_s > 0.95$ are marked with red crosses; non-excluded points are shown as green plusses.

Appendix A. Lepton isolation

The baseline electrons are required to be *Loose* (or *FCLoose* – "Fixed Cut Loose"). The signal ones are *tight*, and for $p_T < 200$ GeV, and *additionally FCHighPtCaloOnly* for higher p_T. These are described in [11] page 37:

$$\begin{aligned} FCLoose: &\quad E_T^{\mathrm{cone20}}/p_T < 0.2, \quad p_T^{\mathrm{varcone20}}/p_T < 0.15, \\ Tight: &\quad E_T^{\mathrm{cone20}}/p_T < 0.06, \quad p_T^{\mathrm{varcone20}}/p_T < 0.06, \\ FCHighPtCaloOnly: &\quad E_T^{\mathrm{cone20}} < \max(0.015 \times p_T, 3.5\mathrm{GeV}). \end{aligned} \tag{A.1}$$

Baseline electrons have $p_T > 7$ GeV, $\eta < 2.47$, no further cuts on these are imposed on the signal.

For the muons, they should be *FCLoose*, described in [10] page 17:

$$p_T^{\mathrm{varcone30}}/p_T^{\mu} < 0.15, \qquad E_T^{\mathrm{topocone20}}/p_T^{\mu} < 0.30. \tag{A.2}$$

Baseline muons are *medium* with $p_T > 6$ GeV, $\eta < 2.7$; the detailed ID criteria for *medium* muons are relevant only to the actual ATLAS experiment and are not given in the paper. Signal muons have $\eta < 2.5$.

The quantities above are defined as:

- $p_T^{\mathrm{varcone30}}$ is the scalar sum of the transverse momenta of he tracks wih $p_T > 1$ GeV in a cone of size $\Delta R = \min(10\ \mathrm{GeV}/p_T^{\mu}, \Delta R_{\mathrm{max}})$, *excluding the electron/muon track itself*, where

$\Delta R_{\max}$ is 0.3 for muons, 0.2 for electrons.
- p_T^{coneXX} is the same but with a fixed cone.
- $E_T^{\text{topocone20}}$ is the sum of the transverse energy in the "topological clusters" in a cone of size $\Delta R = 0.2$ around the muon, after subtracting the energy of the muon itself. I treat this as being the total transverse energy recovered in the given cone.
- E_T^{cone20} is considered to be the same as $E_T^{\text{topocone20}}$ for this analysis.

Appendix B. Pythia settings

The Pythia8 card provided with this analysis gives the A14 tune [19] parameters as well as the filters to select W decays to electrons/muons and Higgs decays to b-quarks. I reproduce them here:

```
24:offIfAny=1 2 3 4 5 6 15 16
25:oneChannel=1 0.5876728 0 -5 5
SigmaProcess:alphaSvalue = 0.140
SpaceShower:pT0Ref = 1.56
SpaceShower:pTmaxFudge = 0.91
SpaceShower:pTdampFudge = 1.05
SpaceShower:alphaSvalue = 0.127
TimeShower:alphaSvalue = 0.127
BeamRemnants:primordialKThard = 1.88
MultipartonInteractions:pT0Ref = 2.09
MultipartonInteractions:alphaSvalue = 0.126
!BeamRemnants:reconnectRange = 1.71
```

The final command appears to be incompatible with the MLM merging and so I comment it out.

References

1. ATLAS Collaboration, G. Aad *et al.* (2020), arXiv:1909.09226 [hep-ex].
2. E. Conte, B. Fuks and G. Serret, *Comput. Phys. Commun.* **184**, 222 (2013), arXiv:1206.1599 [hep-ph].
3. E. Conte and B. Fuks, *Int. J. Mod. Phys.* **A33**, 1830027 (2018), arXiv:1808.00480 [hep-ph].
4. B. Dumont, B. Fuks, S. Kraml, S. Bein, G. Chalons, E. Conte, S. Kulkarni, D. Sengupta and C. Wymant, *Eur. Phys. J.* **C75**, 56 (2015), arXiv:1407.3278 [hep-ph].
5. M. Goodsell, Re-implementation of the H (into b bbar) + 1 lepton + missing transverse momentum analysis (139 fb-1; ATLAS-SUSY-2019-08), https://doi.org/10.14428/DVN/BUN2UX (2020).
6. ATLAS Collaboration, HepData record, https://www.hepdata.net/record/ins1755298.
7. M. Cacciari, G. P. Salam and G. Soyez, *JHEP* **04**, 063 (2008), arXiv:0802.1189 [hep-ph].
8. DELPHES 3 Collaboration, J. de Favereau, C. Delaere, P. Demin, A. Giammanco, V. Lemaître, A. Mertens and M. Selvaggi, *JHEP* **02**, 057 (2014), arXiv:1307.6346 [hep-ex].
9. M. Cacciari, G. P. Salam and G. Soyez, *Eur. Phys. J.* **C72**, 1896 (2012), arXiv:1111.6097 [hep-ph].
10. ATLAS Collaboration, G. Aad *et al.*, *Eur. Phys. J. C* **76**, 292 (2016), arXiv:1603.05598 [hep-ex].
11. ATLAS Collaboration, G. Aad *et al.*, *JINST* **14**, P12006 (2019), arXiv:1908.00005 [hep-ex].
12. D. R. Tovey, *JHEP* **04**, 034 (2008), arXiv:0802.2879 [hep-ph].
13. G. Polesello and D. R. Tovey, *JHEP* **03**, 030 (2010), arXiv:0910.0174 [hep-ph].
14. C. Degrande, C. Duhr, B. Fuks, D. Grellscheid, O. Mattelaer and T. Reiter, *Comput. Phys. Commun.* **183**, 1201 (2012), arXiv:1108.2040 [hep-ph].
15. N. D. Christensen, P. de Aquino, C. Degrande, C. Duhr, B. Fuks, M. Herquet, F. Maltoni and S. Schumann, *Eur. Phys. J. C* **71**, 1541 (2011), arXiv:0906.2474 [hep-ph].

16. C. Duhr and B. Fuks, *Comput. Phys. Commun.* **182**, 2404 (2011), arXiv:1102.4191 [hep-ph].
17. J. Alwall, R. Frederix, S. Frixione, V. Hirschi, F. Maltoni, O. Mattelaer, H. S. Shao, T. Stelzer, P. Torrielli and M. Zaro, *JHEP* **07**, 079 (2014), arXiv:1405.0301 [hep-ph].
18. T. Sjöstrand, S. Ask, J. R. Christiansen, R. Corke, N. Desai, P. Ilten, S. Mrenna, S. Prestel, C. O. Rasmussen and P. Z. Skands, *Comput. Phys. Commun.* **191**, 159 (2015), arXiv:1410.3012 [hep-ph].
19. (11 2014).
20. L. Lönnblad and S. Prestel, *JHEP* **03**, 166 (2013), arXiv:1211.7278 [hep-ph].
21. M. L. Mangano, M. Moretti, F. Piccinini and M. Treccani, *JHEP* **01**, 013 (2007), arXiv:hep-ph/0611129.
22. J. Alwall, S. de Visscher and F. Maltoni, *JHEP* **02**, 017 (2009), arXiv:0810.5350 [hep-ph].
23. J. Debove, B. Fuks and M. Klasen, *Nucl. Phys. B* **842**, 51 (2011), arXiv:1005.2909 [hep-ph].
24. B. Fuks, M. Klasen, D. R. Lamprea and M. Rothering, *JHEP* **10**, 081 (2012), arXiv:1207.2159 [hep-ph].
25. B. Fuks, M. Klasen, D. R. Lamprea and M. Rothering, *Eur. Phys. J. C* **73**, 2480 (2013), arXiv:1304.0790 [hep-ph].
26. J. Fiaschi and M. Klasen, *Phys. Rev. D* **98**, 055014 (2018), arXiv:1805.11322 [hep-ph].
27. Heinrich, Lukas and Feickert, Matthew and Stark, Giordon, pyhf: v0.5.3, https://doi.org/10.5281/zenodo.1169739 (2020).
28. A. L. Read, *J. Phys.* **G28**, 2693 (2002), [,11(2002)].
29. G. Alguero, S. Kraml and W. Waltenberger (9 2020), arXiv:2009.01809 [hep-ph].
30. M. D. Goodsell, S. Kraml, H. Reyes-González and S. L. Williamson, *SciPost Phys.* **9**, 047 (2020), arXiv:2007.08498 [hep-ph].